Computer aided thermal Stress analysis of orthotopic rotating disc

A THESIS SUBMITTED IN PARTIAL FULFILLMENT OF THE REQUIREMENTS FOR THE DEGREE OF

Bachelor of Technology

In

Mechanical Engineering

By

Jitendra nayak

Mechanical Engineering

National Institute of Technology

Rourkela

2009

National Institute of Technology
Rourkela

CERTIFICATE

This is to certify that the thesis entitled, "computer aided thermal stress analysis of orthotopic rotating disc "submitted by **Mr. JITENDRA NAYAK** in partial fulfilment of the requirements for the award of Bachelor inTechnology Degree in Mechanical **Engineering"** at the National Institute of Technology, Rourkela (Deemed University) is an authentic work carried out by him under my supervision and guidance. To the best of my knowledge, the matter embodied in the thesis has not been submitted to any other University / Institute for the award of any Degree or Diploma.

Prof. N.Kavi
Dept. of Mechanical Engg.
National Institute of technology
Rourkela – 769008

ACKNOWLEDGEMENT

We welcome this opportunity to express our heartfelt gratitude and regards to our project guide ***Prof. N.Kavi***, Department of mechanical Engineering, National Institute of Technology, Rourkela for his superb guidance. He always bestowed parental care upon us and evinced keen interest in solving our problems. An erudite teacher, a magnificent person and a strict disciplinarian, we consider ourselves fortunate to have worked under his supervision.

We are highly grateful to ***Prof R.K.Sahoo***, Head of the department, Mechanical Engineering, NIT Rourkela, for providing necessary facilities during the course of the work.

Date: Jitendra Nayak

N.I.T Rourkela

ABSTRACT

This study deals with stress analysis on orthotropic rotating annular discs subjected to various temperature distributions, such as uniform, linearly increasing and decreasing with radius temperatures. Tangential and radial stresses in a rotating disc under the three different temperature profiles are plotted in figures. With the increasing temperature, the tangential stress component decreases at the inner surface whereas it increases at the outer surface, and the radial stress component reduces gradually for all the temperature distributions. The magnitude of the tangential stress component is higher than that of the radial stress component for all the discs under the lower temperatures of the temperature distributions. But, when the temperature is further increased, the tangential stress component decreases more at the inner surface. The radial displacement is also calculated analytically and has higher value at the outer surface than that of the inner surface for all the temperature distributions, except for radial displacement in the reference temperature.

KEY WORDS: orthotropic disc, rotating disc, stress analysis, thermal stress.

CONTENTS

INTRODUCTION

The analysis of rotating discs is an important topic due to their Numerous practical applications, such as high speed gears, flywheels, Turbine motors, and centrifugal pumps. With increasing demand to achieve high strength to weight ratios, optimizing the geometrical and physical properties of the disc configuration becomes more significant . The load-carrying capacity of the reinforced discs is much higher than that of the traditional isotropic steel discs of the same geometry; in addition, the weight of the former is several times lower.

A closed-form solution for the stress analysis in orthotropic disc and cylinders under pressure can be found in literature [3]. Some thermal stress analysis for bars, beams, composite beams, plates, and cylinders are offered in [4].

On the other hand, in the present study, a thermo-elastic stress analysis is carried out on orthotropic rotating annular discs in the cylindrical coordinate system by using an analytical solution.

Literature survey:

The temperature distribution in a part can cause thermal stress effects (stresses caused by thermal expansion or contraction of the material). Examples of this phenomena include interference fit processes (also called shrink or press fit, where parts are mated by heating one part and keeping the other part cool for easy assembly) and creep (permanent deformation resulting from prolonged application of a stress below the elastic limit, such as the behaviour of metals exposed to elevated temperatures over time).

Thermal stress effects can be simulated by coupling a heat transfer analysis (steady-state or transient) and a structural analysis (static stress with linear or nonlinear material models or Mechanical Event Simulation [MES]). The process consists of two basic steps:

1. a heat transfer analysis is performed to determine the temperature distribution; and
2. the temperature results are directly input as loads in a structural analysis to determine the stress and displacement caused by the temperature loads.

For example, a thermal stress analysis of a heat fin model was performed as follows:

- A steady-state heat transfer analysis was performed to obtain the temperature distribution (see Figure 1).

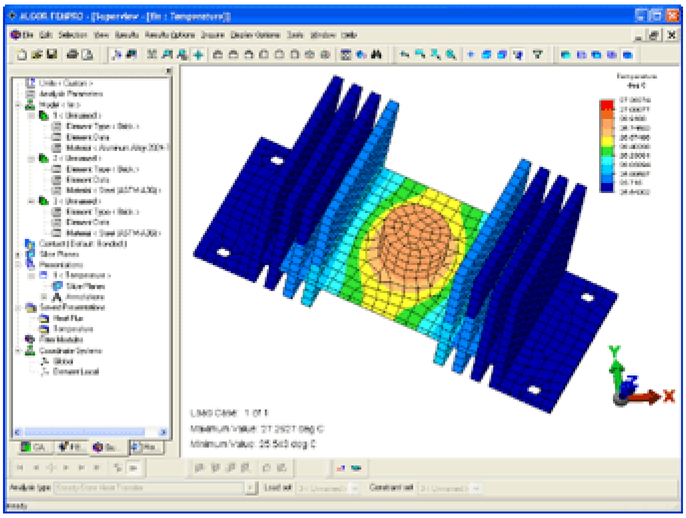

Figure 1: The heat fin model with temperature distribution results from a steady-state heat transfer analysis.

- In the FEA Editor environment of FEMPRO, the analysis type was changed for a structural analysis. In this case, static stress with linear material models was used.
- Constraints were specified for the structural analysis by fully fixing the two bottom surfaces of the model. Additional structural loads (such as forces, pressures and gravity) could have been added if desired; however, for this example, the only loads were the temperatures from the heat transfer analysis.
- On the "Multipliers" tab of the "Analysis Parameters" dialog, a load case multiplier of "1" was specified in the "Thermal" column so that thermal effects would be included in the structural analysis (see Figure 2).

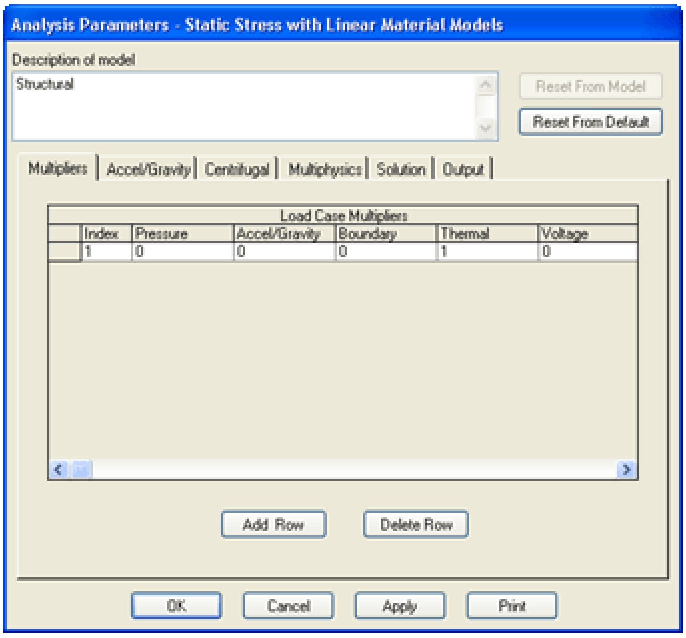

- **Figure 2:** A load case multiplier was specified to include thermal effects in the structural analysis.

On the "Multiphysics" tab of the "Analysis Parameters" dialog, "Steady-state analysis" was chosen from the pull-down menu of options in the "Source of nodal temperatures" field. The "Browse..." button was used to specify the location of the temperature results file from the previous steady-state heat transfer analysis (see Figure 3).

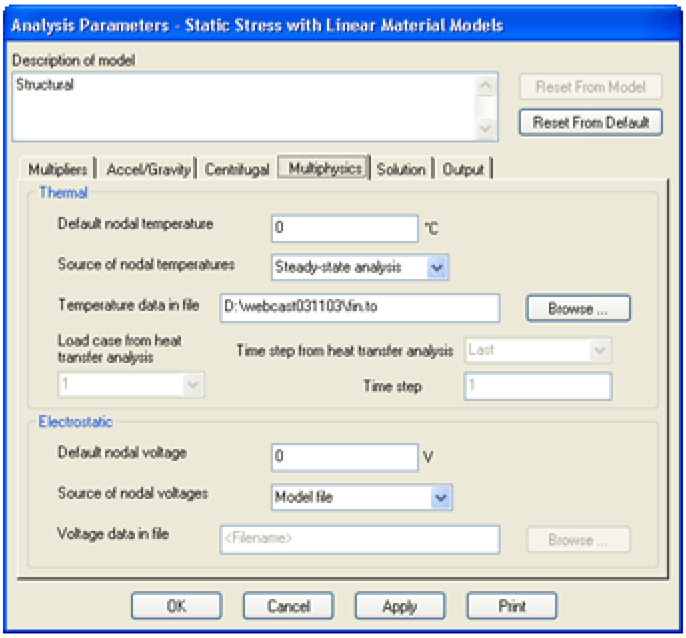

Figure 3: The "Multiphysics" tab of the "Analysis Parameters" dialog was used to specify the temperature results file that would be used as input to the static stress analysis with linear

Materials model

The static stress analysis with linear material models was run and then the results, including thermal stress effects, were displayed in the Superview IV Results environment (see Figure 4).

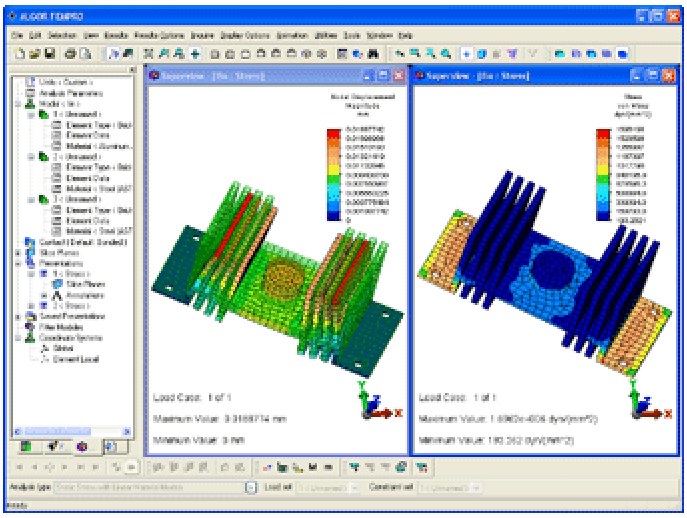

Figure 4: Displacements (left) and stresses (right) in the heat fin model due to temperature loads were displayed in the Superview IV Results environment.

Thus, the ability to couple heat transfer and structural analysis capabilities provides an easy and convenient way to simulate thermal stress effects. To read about one application for thermal stress analysis, see How to Model Initial Strain.

THERMO ELASTIC STRESS ANALYSIS:

The basic differential equation of equilibrium for a rotating disc is

$$\frac{d}{dr}(r\sigma_r) - \sigma_\theta + \rho\omega^2 r^2 = 0 \qquad (1)$$

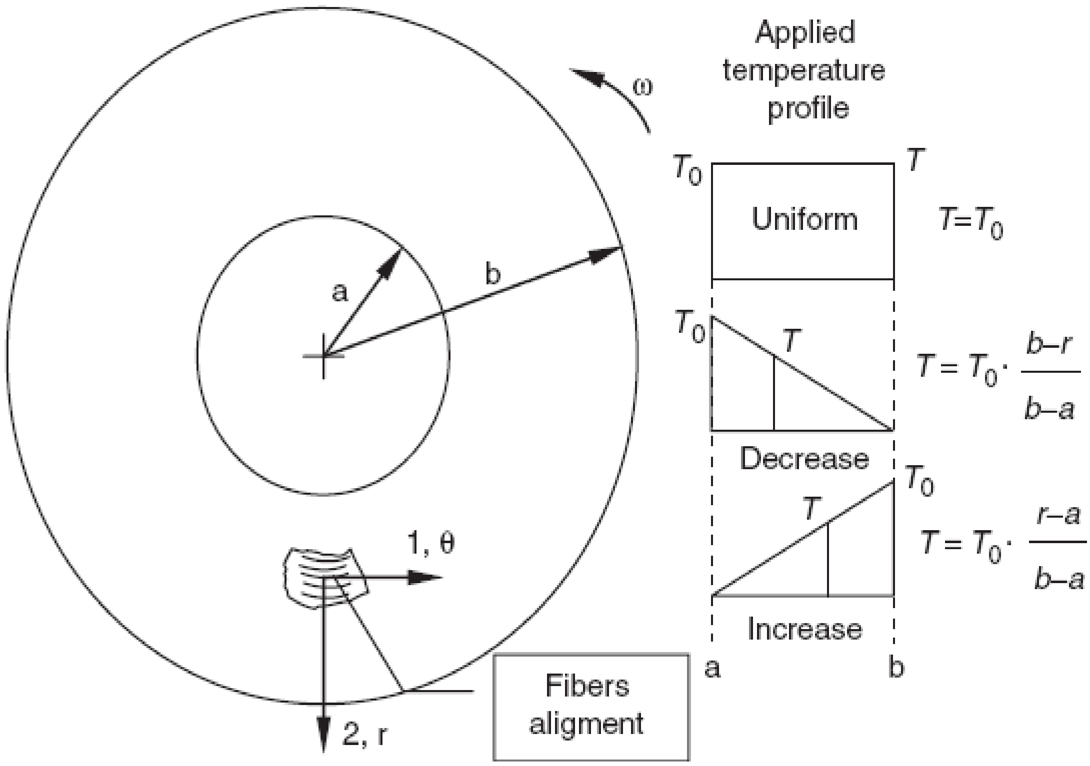

A orthotropic rotating disc under various temperature distributions.

where ρ and ω are the density of the orthotropic material and the angular velocity, respectively.

Owing to the rotational symmetry, the strain–displacement relations are given by

$$\varepsilon_r = \frac{du}{dr}, \quad \varepsilon_\theta = \frac{u}{r} \tag{2}$$

where u is the displacement component in the radial direction, r is the radial distance, r≠0, and r ≤a ≤b, Where a and b are, respectively, inner and outer radii of disc.

The strain compatibility equation is:

$$\frac{d}{dr}(r\varepsilon_\theta) = \varepsilon_{\mathrm{r}}. \tag{3}$$

The strain–stress relation for curvilinearly orthotropic material is:

$$\begin{aligned} \varepsilon_{\mathrm{r}} &= a_{rr}\sigma_r + a_{r\theta}\sigma_\theta + \alpha_{\mathrm{r}} T \\ \varepsilon_\theta &= a_{r\theta}\sigma_r + a_{\theta\theta}\sigma_\theta + \alpha_\theta T \end{aligned} \tag{4}$$

where a_{rr}, $a_{r\theta}$ and $a_{\theta\theta}$ are the components of the compliance matrix and σ_r and σ_θ are the thermal expansion coefficients in the radial and tangential directions. T is the temperature change. $\tau_{r\theta}$ is zero for polarly axisymmetric cases. The equation equilibrium is satisfied by the stress function F defined as:

$$\sigma_r = \frac{F}{r}, \quad \sigma_\theta = \frac{dF}{dr} + \rho\omega^2 r^2. \tag{5}$$

Substituting Equation (5) into Equation (4) gives:

$$\begin{aligned} \varepsilon_r &= \frac{du}{dr} = a_{rr}\frac{F}{r} + a_{r\theta}\left(\frac{dF}{dr} + \rho\omega^2 r^2\right) + \alpha_{\mathrm{r}} T \\ \varepsilon_\theta &= \frac{u}{r} = a_{r\theta}\frac{F}{r} + a_{\theta\theta}\left(\frac{dF}{dr} + \rho\omega^2 r^2\right) + \alpha_\theta T. \end{aligned} \tag{6}$$

Differentiating the second equation and its equal to the former yields the differential equation of the stress function as:

$$r^2 F'' + rF' - \frac{a_{rr}}{a_{\theta\theta}} F = \rho\omega^2 r^3 \left(\frac{a_{r\theta}}{a_{\theta\theta}} - 3 \right) + \frac{(\alpha_r - \alpha_\theta)}{a_{\theta\theta}} rT - \frac{\alpha_\theta}{a_{\theta\theta}} r^2 T'. \qquad (7)$$

The stress function, F, can be obtained by using the transform of $r = e^t$ as:

$$F = C_1 r^k + C_2 r^{-k} + Ar^3 + Br^2 + Cr \qquad (8)$$

where $k^2 = a_{rr}/a_{\theta\theta}$ is the degree of orthotropic, and $k \neq 1$, 2, and 3 for the solution of Equation (8), C_1 and C_2 are the integration constants and the last terms are:

If the orthotropic disc rotates only,

$$A = -\frac{\rho\omega^2}{9 - k^2}(3 + \nu_{\theta r}) \qquad (9a)$$

where $v_{r\theta} = -a_{rr}/a_{\theta\theta}$ is the appropriate Poisson's ratio.

If the rotating disc is subjected to uniform temperature distribution,

$$B = 0$$
$$C = \frac{\alpha_r - \alpha_\theta}{a_{\theta\theta}(1 - k^2)} T_0. \qquad (9b)$$

If the rotating disc is subjected to linearly decreasing function starting from the inside temperature,

$$B = -\frac{\alpha_r - 2\alpha_\theta}{a_{\theta\theta}(4 - k^2)} \frac{1}{b - a} T_0$$
$$C = \frac{\alpha_r - \alpha_\theta}{a_{\theta\theta}(1 - k^2)} \frac{b}{b - a} T_0. \qquad (9c)$$

If the rotating disc is under linearly increasing with radius temperature,

$$B = \frac{\alpha_r - 2\alpha_\theta}{a_{\theta\theta}(4-k^2)} \frac{1}{b-a} T_0$$
$$C = -\frac{\alpha_r - \alpha_\theta}{a_{\theta\theta}(1-k^2)} \frac{a}{b-a} T_0 \qquad (9d)$$

where T_0 is the initial temperature**.**

The stress components can be obtained from the stress function as:

$$\sigma_r = C_1 r^{k-1} + C_2 r^{-k-1} + Ar^2 + Br + C$$
$$\sigma_\theta = kC_1 r^{k-1} - kC_2 r^{-k-1} + 3Ar^2 + 2Br + C + \rho\omega^2 r^2. \qquad (10)$$

The integration constants, C_1 and C_2, can be obtained from the boundary conditionsσ_r is zero at the inner and outer boundaries of the disc (as a mathematical model):

σ_r=0 at r = a and r = b.

By using these conditions, $C_1$and C_2 are determined as:

$$C_1 = \frac{D_2 b^{k+1} - D_1 a^{k+1}}{b^{2k} - a^{2k}}$$
$$C_2 = \frac{D_1 a^{k+1} b^{2k} - D_2 a^{2k} b^{k+1}}{b^{2k} - a^{2k}} \qquad (11)$$

Where

$$D_1 = -(Aa^2 + Ba + C)$$
$$D_2 = -(Ab^2 + Bb + C). \qquad (12)$$

Radial displacement, u, in the elastic solution for small deformation can be determined from Equation (4) as:

$$u = C_1 r^k (a_{r\theta} + k a_{\theta\theta}) + C_2 r^{-k} (a_{r\theta} - k a_{\theta\theta}) + A r^3 (a_{r\theta} + 3 a_{\theta\theta}) + B r^2 (a_{r\theta} + 2 a_{\theta\theta}) + C r (a_{r\theta} + a_{\theta\theta}) + a_{\theta\theta} \rho \omega^2 r^3 + \alpha_\theta T r. \quad (13)$$

RESULTS AND DISCUSSION:

In this study, a thermal stress analysis is carried out on curvilinearly reinforced thermoplastic rotating annular discs subjected to various temperature profiles by using an analytical solution. The thermoplastic material is an injection molded Nylon 6 composite containing 40wt% short glass fiber and its mechanical properties are tabulated in Table 1. The tensile specimens of the thermoplastic material are produced via injection molding and then, the mechanical properties of the specimens are calculated.

The mechanical properties obtained, as seen in Table 1, are utilized in the study. The discs are investigated in the three positions as rotating disc under uniform temperature (Disc 1), linearly decreasing with radius temperature (Disc 2), and linearly increasing with radius temperature (Disc 3). The inner and outer radii, density, and angular velocity of the disc are a=40 mm, b=100 mm, ρ=1.6 g/cm^3, and ω=125 rad/s, respectively. The melting point of the composite material is 280C. It is assumed that the mechanical properties of the disc material are not depended on temperature variation and the thermal stresses are zero at the 0C (reference temperature). When the reference temperature is considered as room temperature, the room temperature should be added to the initial temperature, T0.

While the disc rotates without temperature effect, the radial stress component is found to be maximum according to the radial stress.

Table 1. Mechanical properties of the composite material.

Elasticity moduli (MPa)	E_1	20,000
	E_2	12,000
Shear modulus (MPa)	G_{12}	8000
Poisson's ratio	ν_{12}	0.35
Tensile strength in the fiber direction (MPa)	X	235
Thermal expansion coefficients (1/°C)	α_1	9×10^{-6}
	α_2	114×10^{-6}

component is found to be highest at the inner surface but lowest at the outer surface. Owing to only uniform temperature effect, the radial stress component is zero at the inner and outer surfaces and compressive at each inner section, and the tangential stress component is compressive at the inner points and tensile at the outer points.

Distribution of the tangential and radial stress components along the radial section of the rotating discs for uniform, linearly decreasing and linearly increasing with radius temperature profiles at various temperatures(T_0=0, 50, 100, 150, and 200C) are illustrated in Figures 2–7. The stresses

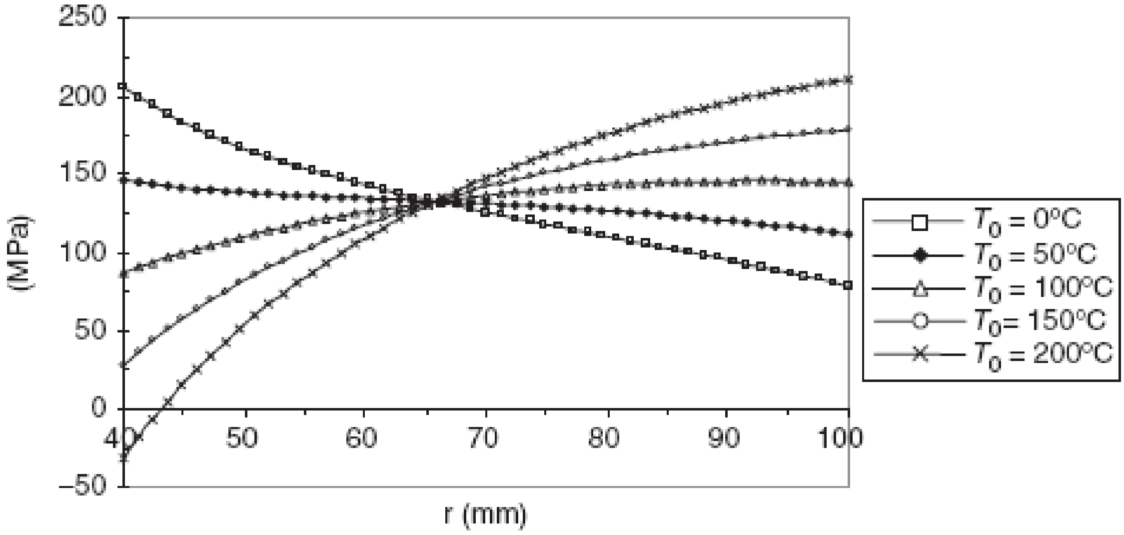

Figure 2. Distributions of the tangential stress components along the radial section of the disc under uniform temperature

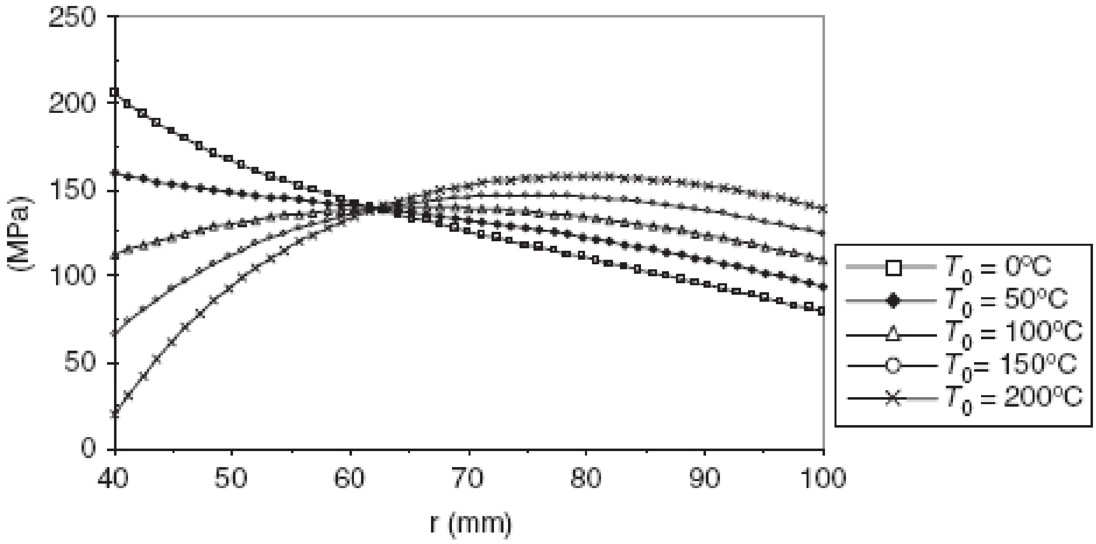

Figure 3. Distributions of the tangential stress components along the radial section of the disc under linearly decreasing temperature with radius

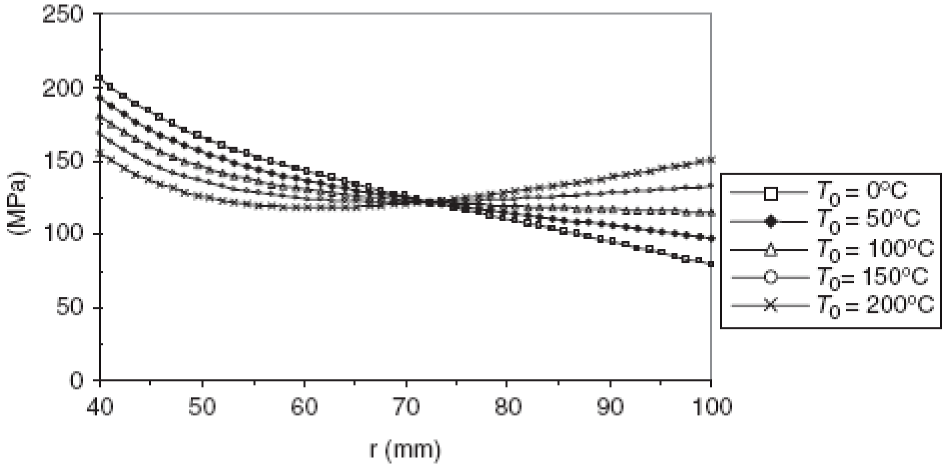

Figure 4. Distributions of the tangential stress components along the radial section of the disc under linearly increasing temperature with radius.

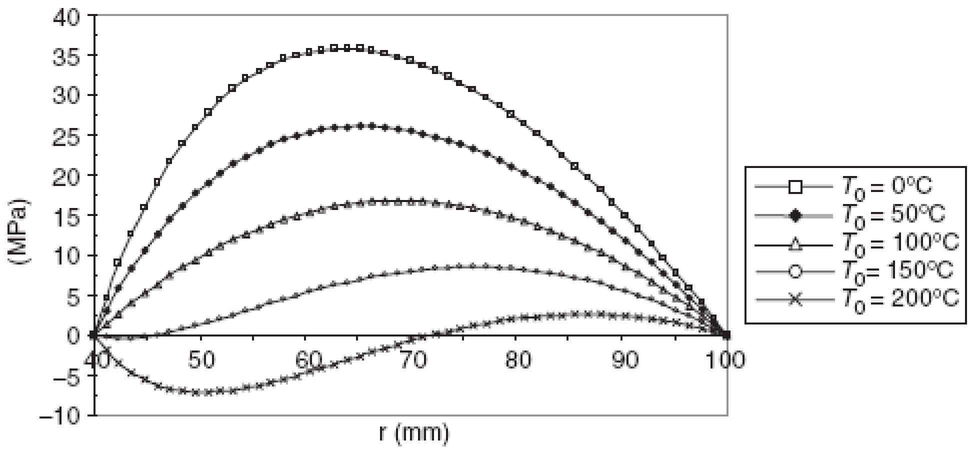

Figure 5. Distributions of the radial stress components along the radial section of the disc under uniform temperature.

which occur from both rotation and thermal loading can be superposed. Thus, when the temperature is increased further the tangential stresses in all the discs go down at the inner points, whereas they go up at the outer points, and the radial stresses always decrease, as seen from the figures. The magnitudes of the tangential stress component are higher than that of the radial stress component. When the stresses in all the discs are compared with each other, the tangential stresses of Disc 1 goes down furthermore at the inner point and goes up furthermore at the outer point, and the radial stresses of Disc 1 goes down furthermore.

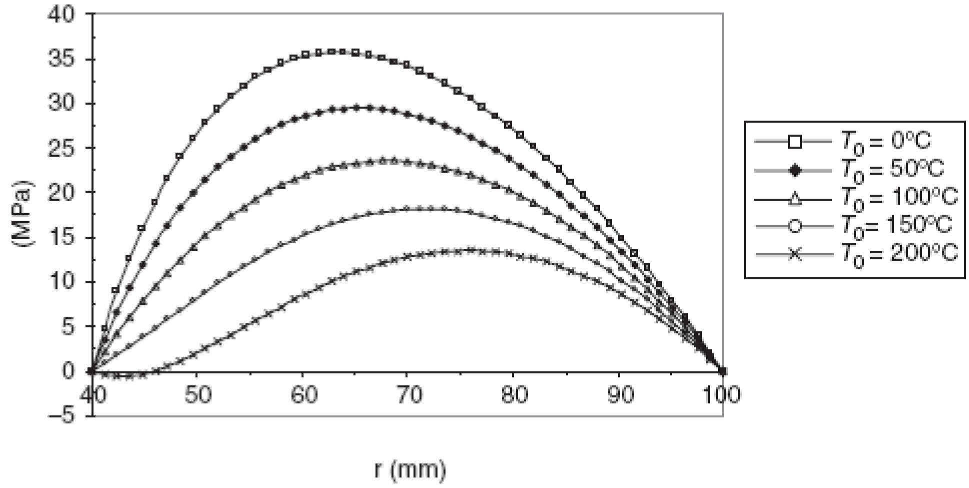

Figure 6. Distributions of the radial stress components along the radial section of the disc under linearly decreasing temperature with radius.

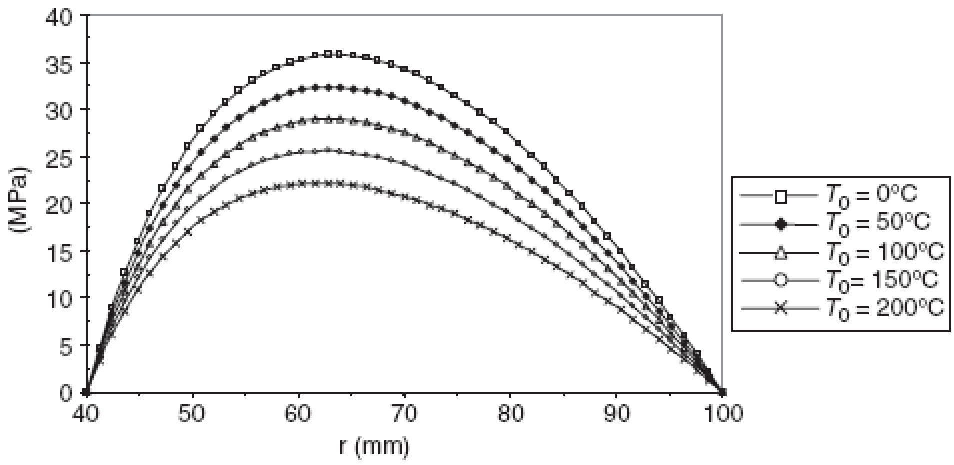

Figure 7. Distributions of the radial stress components along the radial section of the disc under linearly increasing with radius temperature.

The radial and tangential stress values at the inner and outer surfaces in all the discs are given in Table 2. It can be seen that when the temperature is increased further, σ_θ decreases at the inner surface, whereas increases at the outer surface in all the discs. The radial displacements at the inner and outer surfaces are calculated at different temperatures (T_0) and given in Table 3. The radial displacements have higher values at the outer surface than that at the inner surface at other temperatures, except for 0^0 c. It can be seen from this table that the displacements linearly increase or decrease.

Table 2. The radial and tangential stress values at the inner and outer surfaces due to various thermal loading.

		Disc 1	Disc 2	Disc 3	In all the discs	
Temperature (°C)	Surface	σ_θ (MPa)	σ_θ (MPa)	σ_θ (MPa)	σ_r (MPa)	$\tau_{r\theta}$ (MPa)
0	Inner	205.96	205.96	205.96	0.00	0.00
	Outer	78.99	78.99	78.99	0.00	0.00
50	Inner	146.76	159.34	193.38	0.00	0.00
	Outer	111.95	94.04	96.87	0.00	0.00
100	Inner	87.55	112.72	180.79	0.00	0.00
	Outer	144.91	109.14	114.75	0.00	0.00
150	Inner	28.34	66.10	168.20	0.00	0.00
	Outer	177.87	124.22	132.64	0.00	0.00
200	Inner	−30.87	19.48	155.62	0.00	0.00
	Outer	210.83	139.30	150.52	0.00	0.00

Table 3. The radial displacements at the inner and outer surfaces of the discs.

		Disc 1	Disc 2	Disc 3
Temperature (°C)	Surface	*u* (mm)	*u* (mm)	*u* (mm)
0	Inner	0.41	0.41	0.41
	Outer	0.39	0.39	0.39
50	Inner	0.31	0.34	0.39
	Outer	0.60	0.47	0.53
100	Inner	0.21	0.26	0.36
	Outer	0.81	0.55	0.66
150	Inner	0.11	0.19	0.34
	Outer	1.02	0.62	0.80
200	Inner	0.01	0.11	0.31
	Outer	1.23	0.70	0.93

In Figures 8–10, variations of the radial displacements along the radial section of the discs under thermal loading are illustrated. As seen in these figures, while the radial displacements are at first the highest at the inner points and the lowest at the outer points, then, with increasing temperature the radial displacements at the inner sections decrease and those at the outer sections increase further. If the radial displacements in all the discs are compared with each other, the radial displacements in Disc 1 are of the least

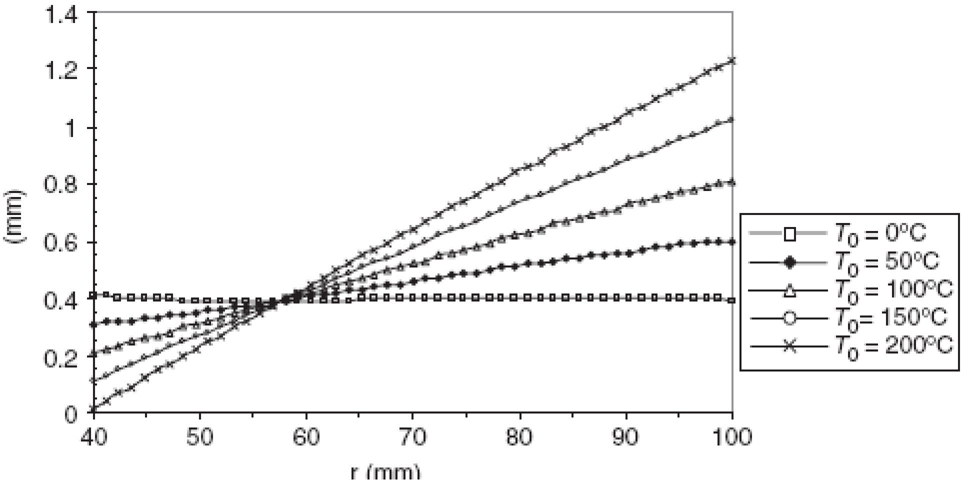

Figure 8. Distributions of the radial displacement along the radial section of the disc under uniform temperature.

value at the inner surfaces, whereas it is of the highest value at the outer surface.

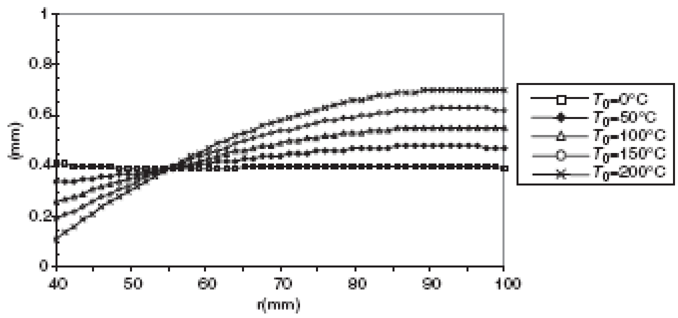

Figure 9. Distributions of the radial displacement along the radial section of the disc under linearly decreasing temperature with radius..

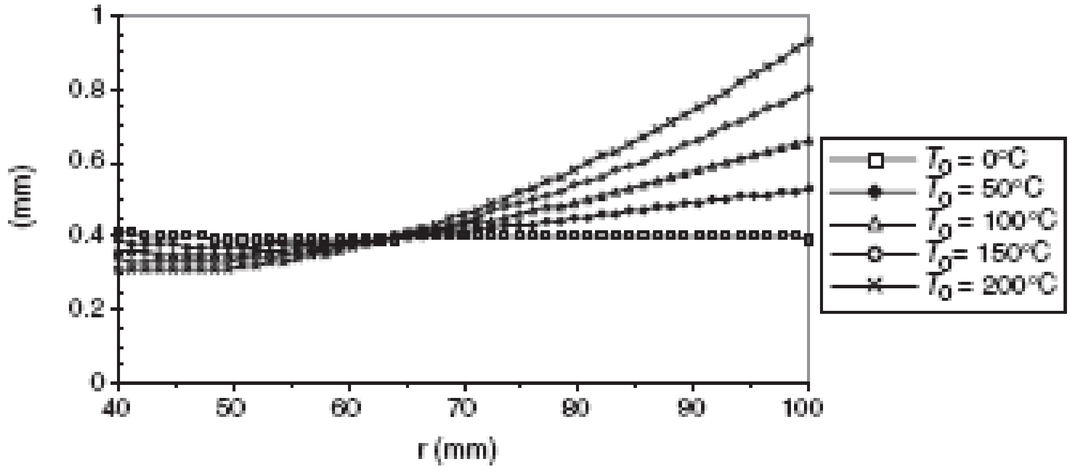

Figure 10. Distributions of the radial displacement along the radial section of the disc under linearly increasing temperature with radius.

CONCLUSION:

1. The tangential stress component is found to be highest at the inner surface but lowest at the outer surface. It, respectively, goes down and up gradually at the inner and outer surfaces by increasing temperature for all the discs.

2. Radial stress component decreases along the radial section when the temperature is increased. The radial stresses may be even become negative around the inner surface.

3. The magnitude of the tangential stress is higher than that of the radial Stress.

4. The analytical solution gives the radial displacement component at each point. The radial displacement decreases and increases at the inner and outer surfaces, respectively, for all the temperature profiles.

5. While the radial displacements are at first higher at the inner points and lower at the outer points, then the radial displacements decrease at the inner sections whereas increase further at the outer sections by increasing temperature for all the discs.

REFERENCES:

1. Jain, R., Ramachandra, K. and Simha, K.R.Y. (1999). Rotating Anisotropic Disc of Uniform Strength, Int. J. Mechanical Sciences, 41: 639–648.
2. Nemirovskii, Y.V. and Yankovskii, A.P. (2002). Rational Profiling of Reinforced Rotating Disks, Mechanics of Composite Materials, 38(1): 1–15.
3. Lekhnitskii, S.G. (1981). Theory of Elasticity of an Anisotropic Body, Mir Publishers,
Moscow.

4.Noda, N., Hetnarski, R.B. and Tanigava, Y. (2000). Thermal Stresses, Lastran Corporation.

5. Genta, G. and Gola, M. (1981). The Stress Distribution in Orthotropic Rotating Disks, J. Applied Mechanics, 48: 559–562.
6. Jain, R., Ramachandra, K. and Simha, K.R.Y. (2000). Singularity in Rotating Orthotropic Discs and Shells, Int. J. Solids and Structures, 37: 2035–2058.
7. Stanley, P. and Garroch, C. (1999). A Thermoelastic Disc Test for the Mechanical Characterization of Fibre-Reinforced Moulded Composites: Theory, Composites Science &
Technology, 59: 371–378.
8. Sing, S.B. and Ray, S. (2002). Modeling the Anisotropy and Creep in Orthotropic Aluminum-Silicon Carbide Composite Rotating Disc, Mechanics of Materials, 34: 363–372.
9. Tutuncu, N. (1995). Effect of Anisotropy on Stresses in Rotating Discs, Int. J. Mechanical Science, 37(8): 873–881.